

Batch correction of high-dimensional data

Emanuele Aliverti¹, Jeff Tilson², Dayne Filer^{2,3}, Benjamin Babcock^{3,4}, Alejandro Colaneri³, Jennifer Ocasio^{4,5}, Timothy R. Gershon^{4,5,6,7}, Kirk C. Wilhelmsen^{2,3,4}, and David B. Dunson⁸

¹Department of Statistical Sciences, University of Padova, Padova

²RENCI, Chapel Hill, NC 27517 USA

³Department of Genetics, University of North Carolina School of Medicine, Chapel Hill

⁴Department of Neurology, University of North Carolina School of Medicine, Chapel Hill

⁵UNC Neuroscience Center, University of North Carolina School of Medicine, Chapel Hill

⁶Carolina Institute for Developmental Disabilities, University of North Carolina School of Medicine, Chapel Hill

⁷Lineberger Comprehensive Cancer Center, University of North Carolina School of Medicine, Chapel Hill

⁸Department of Statistical Science, Duke University, Durham

Abstract

Motivation: Biomedical research often produces high-dimensional data confounded by batch effects such as systematic experimental variations, different protocols and subject identifiers. Without proper correction, low-dimensional representation of high-dimensional data might encode and reproduce the same systematic variations observed in the original data, and compromise the interpretation of the results. In this article, we propose a novel procedure to remove batch effects from low-dimensional embeddings obtained with *t*-SNE dimensionality reduction.

Results: The proposed methods are based on linear algebra and constrained optimization, leading to efficient algorithms and fast computation in many high-dimensional settings. Results on artificial single-cell transcription profiling data show that the proposed procedure successfully removes multiple batch effects from *t*-SNE embeddings, while retaining fundamental information on cell types. When applied to single-cell gene expression data to investigate mouse medulloblastoma, the proposed method successfully removes batches related with mice identifiers and the date of the experiment, while preserving clusters of oligodendrocytes, astrocytes, and endothelial cells and microglia, which are expected to lie in the stroma within or adjacent to the tumors.

Availability: Source code implementing the proposed approach in R and julia is available at the link https://github.com/emanuelealiverti/BC_tSNE, including a tutorial to reproduce the simulation studies.

1 INTRODUCTION

Recent technological improvements in transcriptome analysis provide many valuable insights on complex biological systems, with single-cell RNA transcription profiling (scRNAseq) analysis being one of the most popular tools to investigate intricate cellular processes (Hwang et al., 2018). A fundamental goal in scRNAseq is to cluster cells into different groups, in order to detect different cell types and different cell cycles, such as progenitors or cells in differentiated states (e.g., Johnson et al., 2007). To address such an aim, investigators produce compact low-dimensional representations of high-dimensional scRNAseq data, visualizing the expression matrix in two dimensions and identifying potential clusters via visual inspection or with appropriate clustering algorithms.

A large variety of methods for linear and non-linear dimensionality reduction and data visualisation are available, with t -distributed Stochastic Neighbor Embedding (t -SNE, Maaten and Hinton, 2008) being of great utility in analyzing scRNAseq data. Unfortunately, visualization by t -SNE and other methods to perform dimensionality reduction can be strongly biased by nuisance covariates and batch effects. Such covariates may include the batches due to different devices used for an experiment, the length of time from dissociation cells until library preparation, and even gender of the subject (e.g. Luo et al., 2010). Without adjustment, variation in the low-dimensional summaries may be driven by nuisance covariates instead of the primary factors of scientific interest — such as cell types — suggesting artificial separation due to such “nuisance” covariates. Although some unwanted associations can be minimised with more careful experimental design, many batch effects are unavoidable; for example, when a different experimental setup is used for each biological sample (Luo et al., 2010).

The focus of this article is on producing simple batch-corrected modifications of t -SNE that can be used to easily remove associations with multiple batches. Our methods are based on linear algebra results and modification of gradient descent optimisation, therefore providing simple and scalable tools to remove batch effects in many complex settings.

Various methods for removing batch effects are available in the literature, with methods based on matrix decomposition being very popular in genomics (e.g. Wall et al., 2003). Alter et al. (2000) use Singular Value Decomposition (SVD) of the original expression matrix to filter out the singular vector associated with systematic and non-experimental variations, and reconstruct an adjusted expression matrix with the remaining singular vectors. A similar strategy was pursued in Bylesjö et al. (2007), where the main focus was on separating the latent structures of the expression matrix that are not affected by batch assignment. Leek and Storey (2007) combine SVD decomposition and linear modelling to remove the effect of unwanted variations and detect eigengenes that are differentially expressed. Model-based methods have also demonstrated utility; for example, distance discrimination based on Support Vector Machines (Benito et al., 2004) and multilevel models (Johnson et al., 2007). For a more comprehensive review of approaches for batch correction and array normalization, see Luo et al. (2010), Lazar et al. (2012), and Scherer (2009). Although these methods provide effective tools for reducing batch effects in

high-dimensional scRNAseq arrays, little attention has been devoted to removing batches from t -SNE embeddings. More precisely, t -SNE is widely used as a tool for assessing the success in removing such unwanted associations, but a formal procedure which attempts to directly estimate t -SNE embeddings that are not driven by systematic biases is still lacking.

We take a step toward addressing this goal, focusing on the development of a novel procedure to obtain an adjusted t -SNE low-dimensional representation that removes batch effects without affecting factors of scientific interest. Our procedure is developed leveraging two main steps, with the first one focusing on removing batches with linear effects in the original data, and the second on developing a projected gradient descent algorithm to estimate t -SNE embeddings and guarantee that also non-linear transformation of the data will be uncorrelated with such batches. The proposed approach is empirically evaluated on artificial scRNAseq data, and further applied to gene expression data to investigate mouse medulloblastoma.

2 METHODS

2.1 Notation & problem formulation

Consider a data matrix $\mathbf{X} = \{\mathbf{x}_i^T\}_{i=1}^n$ with observations $\mathbf{x}_i = (x_{i1}, \dots, x_{ip})$. In many biological applications, the number of features p is tremendously large and it is of interest to provide accurate low-dimensional representation of such high dimensional data. Dimensionality reduction techniques focus on finding low-dimensional counterparts $\mathbf{y}_i = (y_{i1}, \dots, y_{iq})$ of each \mathbf{x}_i , preserving as much structure as possible with $q \ll p$ components; generally, $q = 2$ or $q = 3$ for the ease of graphical visualisation. Original observations \mathbf{x}_i can potentially lie in a complex and highly non-linear manifold; for example, wrapped spaces such as rolls (e.g [Lee and Verleysen, 2005](#)). In contrast, the desired low-dimensional embedding lie on a standard q -dimensional Euclidean space, and \mathbf{y}_i determines the position of observation i in such an embedded space.

Low-dimensional representations are constructed in order to preserve some specific structure of the original data; some examples include preserving Euclidean distances (Multidimensional Scaling, [Kruskal, 1964](#)), variances (Principal Component Analysis), neighborhood graphs (Local Linear Embedding and Isomap, [Roweis and Saul, 2000](#); [Tenenbaum et al., 2000](#)) or local similarities among points (Stochastic Neighbor Embedding, [Hinton and Roweis, 2003](#)). Many methods estimate an explicit function between the original data and their embeddings; for example, the PCA solution is a linear combination of the columns of \mathbf{X} . More recently, focus has shifted to obtaining \mathbf{y}_i without explicitly defining such a map, thus allowing a greater flexibility and range of application. In this article, we focus on the t -SNE methodology for dimensionality reduction and data visualisation ([Maaten and Hinton, 2008](#)). t -SNE attempts to find low-dimensional representations that preserve local similarities among data points, with similarities parameterized as conditional probabilities of belonging to the same local neighborhood. In the following paragraphs, we review the standard formulation of t -SNE before introducing our adjustments for batch effects.

2.2 Standard t -SNE algorithm

In the original input space, t -SNE defines dissimilarities among points as symmetric probabilities $p_{ij} = (p_{i|j} + p_{j|i})/2n$, with

$$p_{i|j} = \frac{\exp(-0.5\|\mathbf{x}_i - \mathbf{x}_j\|^2/\sigma_i^2)}{\sum_{k, k \neq i} \exp(-0.5\|\mathbf{x}_i - \mathbf{x}_k\|^2/\sigma_i^2)}. \quad (1)$$

Equation 1 can be interpreted as the probability that point i picks j as its neighbor, under a Gaussian kernel centered at \mathbf{x}_i and with standard deviation equal to σ_i . The intuition behind the introduction of p_{ij} comes from averaging $p_{i|j}$ and $p_{j|i}$ to reduce the relative impact of outliers and define a symmetric dissimilarity metric (Maaten and Hinton, 2008). The parameter σ_i^2 determines the width of the Gaussian kernel and, indirectly, the number of local neighbors associated with each point i , with $i = 1, \dots, n$. Defining σ_i^2 is a primary step in producing t -SNE embeddings, with the selection determining the *perplexity* of the resulting distribution (Maaten and Hinton, 2008; Hinton and Roweis, 2003). Large values of σ_i^2 correspond to a larger number of local neighbors and greater perplexity, while default values of perplexity range in the interval $\{10, 50\}$ (Maaten and Hinton, 2008). Embeddings generally show robustness to moderate changes in perplexity (Maaten, 2014).

Dissimilarity among points \mathbf{y}_i in the embedded space is defined through the kernel of a t -distribution with 1 degree of freedom, setting

$$q_{ij} = \frac{(1 + \|\mathbf{y}_i - \mathbf{y}_j\|^2)^{-1}}{\sum_{k, k \neq i} (1 + \|\mathbf{y}_i - \mathbf{y}_k\|^2)^{-1}}. \quad (2)$$

The t -SNE embeddings \mathbf{y}_i are selected minimizing the Kullback-Leibler divergence between p_{ij} and q_{ij} ; note that p_{ij} does not depend on \mathbf{y} and is a fixed value given the input data. Let $\mathbf{y} = (\mathbf{y}_1, \dots, \mathbf{y}_n)$ and highlight the dependency of q_{ij} on the embeddings \mathbf{y} in Equation 2 as $q_{ij}(\mathbf{y})$. Formally, t -SNE is the solution to the following optimisation problem.

$$\underset{\mathbf{y}}{\operatorname{argmin}} \{L(\mathbf{y})\} = \underset{\mathbf{y}}{\operatorname{argmin}} = \left\{ \sum_{i=2}^n \sum_{j=1}^i p_{ij} \log \frac{p_{ij}}{q_{ij}(\mathbf{y})} \right\} \quad (3)$$

The objective function $L(\mathbf{y})$ can be optimized through gradient methods. Indeed, the partial derivative of the loss functions in Equation 3 with respect to \mathbf{y}_i is equal to

$$\begin{aligned} \nabla L(\mathbf{y}_i) &= \frac{\partial L}{\partial \mathbf{y}_i} = 4 \sum_{\substack{j=1 \\ j \neq i}}^n (p_{ij} - q_{ij}) q_{ij} Z(\mathbf{y}_i - \mathbf{y}_j); \\ Z &= \sum_{l \neq k} (1 + \|\mathbf{y}_l - \mathbf{y}_k\|^2)^{-1}; \end{aligned} \quad (4)$$

see Maaten and Hinton (2008, Appendix A) for the complete derivation.

Therefore, the generic gradient descent step with momentum correction for updating \mathbf{y}_i at iteration $t + 1$ sets

$$\mathbf{y}_i^{(t+1)} = \mathbf{y}_i^{(t)} + \eta^{(t)} \nabla L(\mathbf{y}_i^{(t)}) + \alpha^{(t)} (\mathbf{y}_i^{(t)} - \mathbf{y}_i^{(t-1)}), \quad (5)$$

with $\eta^{(t)}$ indicating the learning rate and $\alpha^{(t)}$ the momentum term; see [Maaten and Hinton \(2008\)](#) for practical advices on the choice of such functions.

2.3 Batch-corrected t -SNE

Let \mathbf{Z} denote an additional variable which contains batch information. We refer to the proposed method as BC- t -SNE (Batch-Corrected t -SNE) in the sequel. When the number of features p is extremely large and when it exceeds the number of observations n , direct application of t -SNE on the raw data \mathbf{X} can be challenging, computationally inefficient, and lead to poor results. Therefore, it is generally advised to perform a preliminary dimensionality reduction, and then apply t -SNE over such reduced representation to improve the results ([Maaten, 2014](#)). For example, default software implementation estimates t -SNE embeddings on the first k principal components, with k in the range $[30 - 50]$ (e.g. [Pedregosa et al., 2011](#)). Reducing the dimensionality from p to k speeds up computation and reduces noise without affecting local similarities among observations ([Maaten and Hinton, 2008](#)).

The first step of BC- t -SNE is motivated by the above considerations, and focuses on processing the data with the approach introduced in [Aliverti et al. \(2018\)](#) to explicitly obtain the optimal low-rank approximation of a matrix \mathbf{X} in Frobenius norm under an orthogonality constraint between such approximation and the batch variable \mathbf{Z} . Therefore, the method removes linear effects between the reduced data and the variables in \mathbf{Z} with minimal information loss. Such an approach is based on computing the residuals from a multivariate regression among the left singular vectors of \mathbf{X} and \mathbf{Z} , and is therefore comparable with standard PCA in terms of computational requirements, providing a practical alternative to perform dimensionality reduction while simultaneously achieving batch removal. Although such a procedure is optimal in removing the linear influence of batches, effects beyond linearity might still affect t -SNE embeddings. In practical applications such higher order effects are often small in magnitude, and second order adjustment often lead to satisfactory results in terms of batch-correction (e.g. [Aliverti et al., 2018](#)). However, since the t -SNE embeddings \mathbf{y}_i are a complex non-linear functional of the original \mathbf{x}_i , inclusion of higher-order constraints provides a reasonable conservative choice.

The second step of BC- t -SNE adjustment can be better motivated by introducing some details on gradient descent, which can be interpreted as an optimisation to minimize the linearisation of the loss function (Kullback-Leibler divergence for t -SNE) around the current estimates, including a smoothing penalty that penalises abrupt changes (e.g. [Hastie et al., 2015](#)). To see that, consider the gradient descent step in Equation 5, setting without loss of generality $\alpha^{(t)} = 0$. The following alternative representation holds.

$$\mathbf{y}_i^{(t+1)} = \operatorname{argmin}_{\mathbf{y}_i \in \mathbb{R}^q} \left\{ L(\mathbf{y}_i^{(t)}) + \langle \nabla L(\mathbf{y}_i^{(t)}), \mathbf{y}_i - \mathbf{y}_i^{(t)} \rangle - \frac{1}{\eta^{(t)}} \|\mathbf{y}_i - \mathbf{y}_i^{(t)}\|_2^2 \right\}. \quad (6)$$

This view of gradient descent facilitates the introduction of further constraints. Indeed, this aim is achieved by restricting the solution $\mathbf{y}_i \in \mathcal{C}$, with \mathcal{C} denoting a constrained region of the original space \mathbb{R}^q . Such a constraint can

Algorithm 1: Batch-corrected t -SNE with projected gradient

Apply OG (Aliverti et al., 2018) to extract the first k components of \mathbf{X} and remove linear batch effects. Denote the $n \times k$ reduced and adjusted matrix as $\hat{\mathbf{X}}$ **for** $i = 1, \dots, n$ **do**

- | Perform binary search to find the value σ_i^2 that achieves desired level of *perplexity* (Maaten and Hinton, 2008)

end

Compute the pairwise similarities p_{ij} in Equation 1 from $\hat{\mathbf{X}}$ and $\{\sigma_i^2\}_{i=1}^n$ **for** $t = 1, \dots, T$ **do**

- | Compute affinities q_{ij} defined in Equation 2 **for** $i = 1, \dots, n$ **do**
- | | Update $\mathbf{y}_i^{(t+1)}$ (the i -th row of $\mathbf{Y}^{(t+1)}$) as
- | | |
$$\mathbf{y}_i^{(t+1)} = \mathbf{y}_i^{(t)} + \eta^{(t)} \nabla L(\mathbf{y}_i^{(t)}) + \alpha^{(t)} (\mathbf{y}_i^{(t)} - \mathbf{y}_i^{(t-1)})$$
- | | **end**
- | Compute $\boldsymbol{\beta}^{(t+1)} \leftarrow \text{solve}(\mathbf{Z}^\top \mathbf{Z}, \mathbf{Z}^\top \mathbf{Y}^{(t+1)})$ Compute projected gradient update, setting
- | |
$$\tilde{\mathbf{Y}}^{(t+1)} = \mathbf{Y}^{(t+1)} - \mathbf{Z} \boldsymbol{\beta}^{(t+1)}$$

end

Output: Return $\tilde{\mathbf{Y}}^{(T)}$.

be easily imposed by performing a standard gradient step, and then projecting the result back into the constrained set \mathcal{C} , leading to a procedure referred to as *projected* gradient descent; see, for example, Hastie et al. (2015, Sec 5.3.2) for further details. The choice of the constrained set \mathcal{C} covers a central role in the optimisation, since the projection should be computed easily in order to make the method practical in high-dimensional applications. With this motivation in mind, we propose a computationally simple solution and restrict $\mathbf{Y} = \{\mathbf{y}_i^\top\}_{i=1}^n$ such that it is orthogonal with the subspace spanned by the columns of \mathbf{Z} . This constraint can be easily imposed with linear regression, computing at each iteration a projected gradient step which constructs an update $\tilde{\mathbf{Y}}^{(t+1)}$ that projects the unconstrained solution $\mathbf{Y}^{(t+1)}$, making it orthogonal with the batch variables \mathbf{Z} . Pseudo-code illustrating the method is reported in Algorithm 1. A julia implementation is available at the link https://github.com/emanuelealiverti/BC_tSNE.

3 SIMULATION STUDY

A simulation study is conducted to evaluate the performance of the proposed method on artificial scRNAseq data. Artificial single-cell RNA sequencing data were generated with the BioConductor library splatter, which provides an interface to create complex datasets with several realistic features (Zappia et al., 2018). Specifically, a dataset consisting of $p = 10000$ genes measured over $n = 800$ cells was generated with 4 batch effects and 4 different cell types. A complete tutorial to reproduce the artificial data and simulation study in R and julia is available at the link https://github.com/emanuelealiverti/BC_tSNE.

The focus of the simulation is on assessing the success of BC- t -SNE at removing unwanted associations while retaining information of the scientific factors of interest, which correspond to cell types in this particular example. The adjusted approach is also compared with a standard implementation of t -SNE, available with R package Rtsne

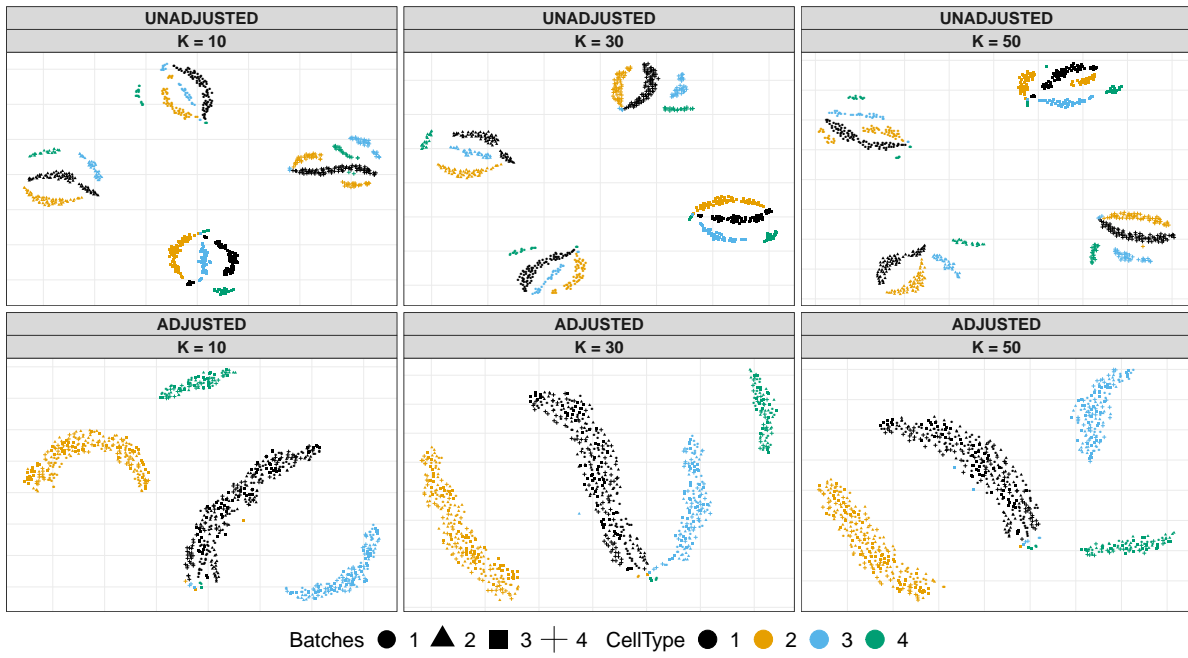


Figure 1: Simulation study. The color of points varies according to cell types, while shapes vary with batch groups. Upper plot shows the unadjusted t -SNE coordinates, while results for BC- t -SNE are reported in the bottom panels.

(Krijthe, 2015). In order to properly compare the two methods, parameters of BC- t -SNE were fixed to the default configuration of the package Rtsne, which corresponds to setting the number of iterations $T = 1000$, a value of perplexity equal to 30 and $\eta^{(t)} = 200, t = 1, \dots, T$ and $\alpha^{(t)} = 0.5$ for $t < 250$ and $\alpha^{(t)} = 0.8$ for $t \geq 250$; see also Maaten and Hinton (2008).

Figure 1 compares results from unadjusted t -SNE and the proposed method, respectively in the upper and lower panels; both approaches are estimated over a set of $k = \{10, 30, 50\}$ reduced components. Such a reduction was obtained with PCA for the unadjusted method and with the OG approach of Aliverti et al. (2018) for BC- t -SNE, as illustrated in step 2 of Algorithm 1. Results for the unadjusted case effectively illustrate a realistic situation where batch effects might be highly misleading for data exploration. Indeed, cells are divided into 4 main clusters corresponding to the different batches, denoted with different point shapes. Within each cluster, smaller groups of cells of the same type are present; however, it is clear that the main clusters are driven by batch information instead of cell types. Therefore, results from the upper panel of Figure 1 do not allow us to properly identify regions of the space or partitions which are consistent with the factors of scientific interest. The bottom panels of Figure 1 illustrate results for BC- t -SNE and show that, after adjustment, the effect of unwanted batches is completely removed from the t -SNE embeddings. Indeed, different point shapes are uniformly spread across the four main clusters, which now correspond to the different cell types denoted with different colors.

4 APPLICATION

4.1 Dataset description

Medulloblastoma is among the most frequent malignant brain tumors in children. Recent studies have observed that the Sonic Hedgehog (SHH) signaling pathway is hyperactivated in 30% of human medulloblastoma, therefore stimulating novel studies in this direction (Zurawel et al., 2000; Ellison et al., 2011). Activation of the SHH pathway, which stimulates proliferation of granule cell neurons during cerebellar development, has been used to create genetically engineered mice for scientific purposes, with the SmoM2 process being a routinely used pipeline (Rubin and de Sauvage, 2006). Specifically, SmoM2 mice have a transgenic mutated Smo allele which was originally isolated from a tumor and can be engineered to be not expressed until acted upon by Cre recombinase (Mao et al., 2006; Helms et al., 2000; Machold and Fishell, 2005). These mice are mated with genetically engineered matches that express Cre recombinase in cerebellar granular neuron progenitors, leading to descendants which develop medulloblastoma with 100% frequency by postnatal day 12.

Data used in this section comes from 5 mice created using such a pipeline. Tumors were dissociated and individual cells co-encapsulated in a microfluidics chamber with primer-coated beads in oil-suspended droplets. All primers on each bead contained a bead-specific bar code and an unique molecular identifier (UMI), followed by an oligo-dT sequence, while mRNAs were captured on the oligo-dT, reverse-transcribed and amplified. Libraries were generated using the Drop-seq protocol V3.1 (Macosko et al., 2015). Following standard sequencing procedures, individual transcripts were identified by the UMI bar code, with cell identity inferred from the bead-specific bar codes.

Analysis has been restricted to cells with more than 500 detected genes. Furthermore, outlier cells with more than 4 standard deviations above the median number of genes were excluded from the analysis, along with UMIs and mitochondrial content per cell in order to address the common problems of gene drop out, unintentional cell-cell multiplexing and premature cell lysis (Vladoiu et al., 2018). The resulting expression matrix \mathbf{X} consists of $p = 16680$ genes measured over $n = 17746$ different cells.

4.2 Results

Using the same settings of the simulations, unadjusted t -SNE embeddings are estimated over the first $k = 50$ and $k = 30$ principal components; larger number of principal components resulted in less structured embeddings, and are not reported. First row of Figure 2 refers to $k = 30$, second row to $k = 50$. In both settings, results suggest the presence of strong batch effects, with respect to mouse identifier (first column), sex of the mice (second column) and date of the experiment (third column). For example, cells from mouse 1 form a cluster which is clearly distinct from the others.

Figure 3 refers to BC- t -SNE coordinates estimated with $k = 30$ and $k = 50$ using Algorithm 1. Results show a satisfactory performance in terms of batch effect removal. Indeed, BC- t -SNE embeddings from Figure 3 shows that

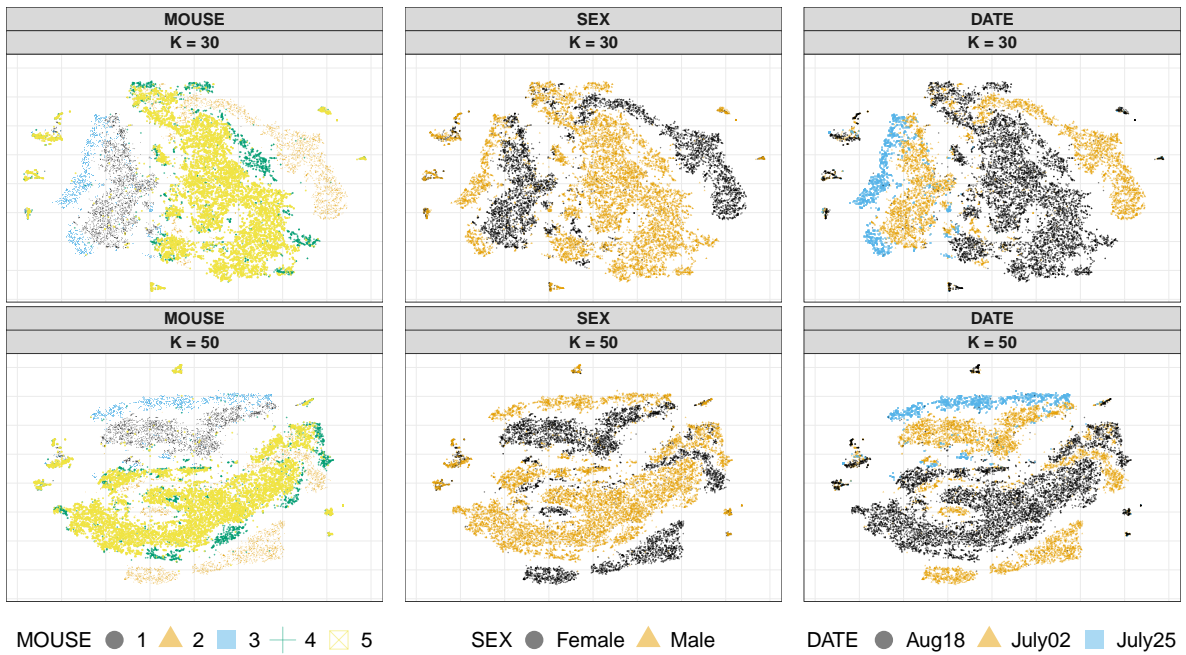


Figure 2: Unadjusted t -SNE coordinates. Points and shapes vary with batches.

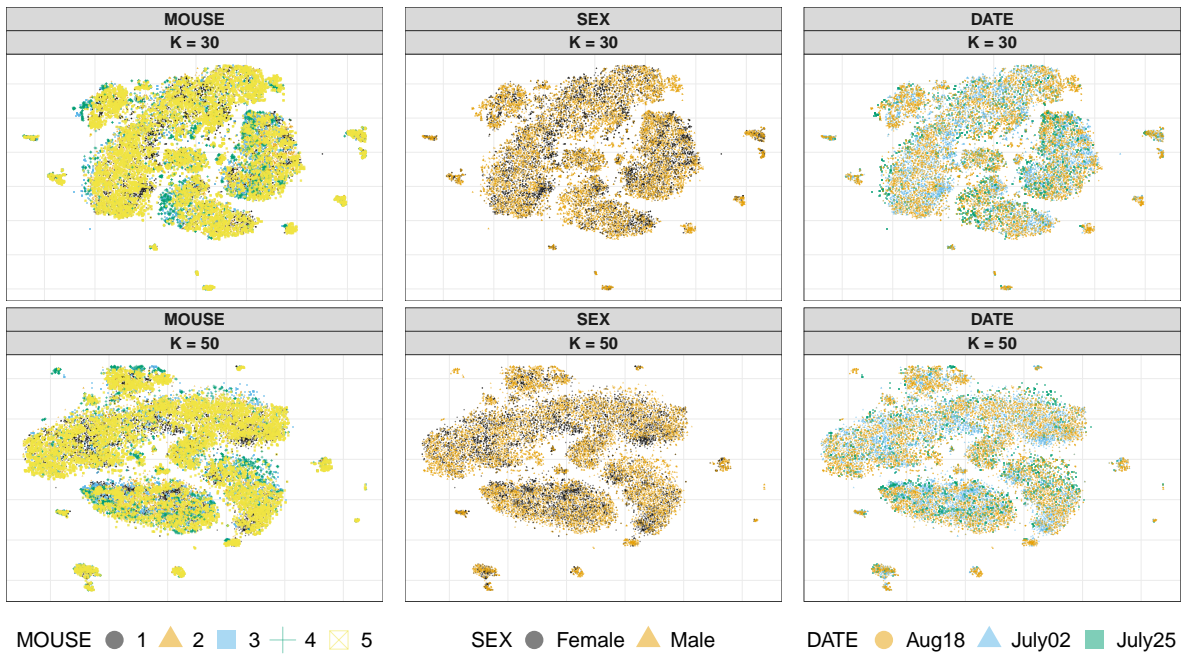


Figure 3: BC- t -SNE coordinates. Points and shapes vary with batches.

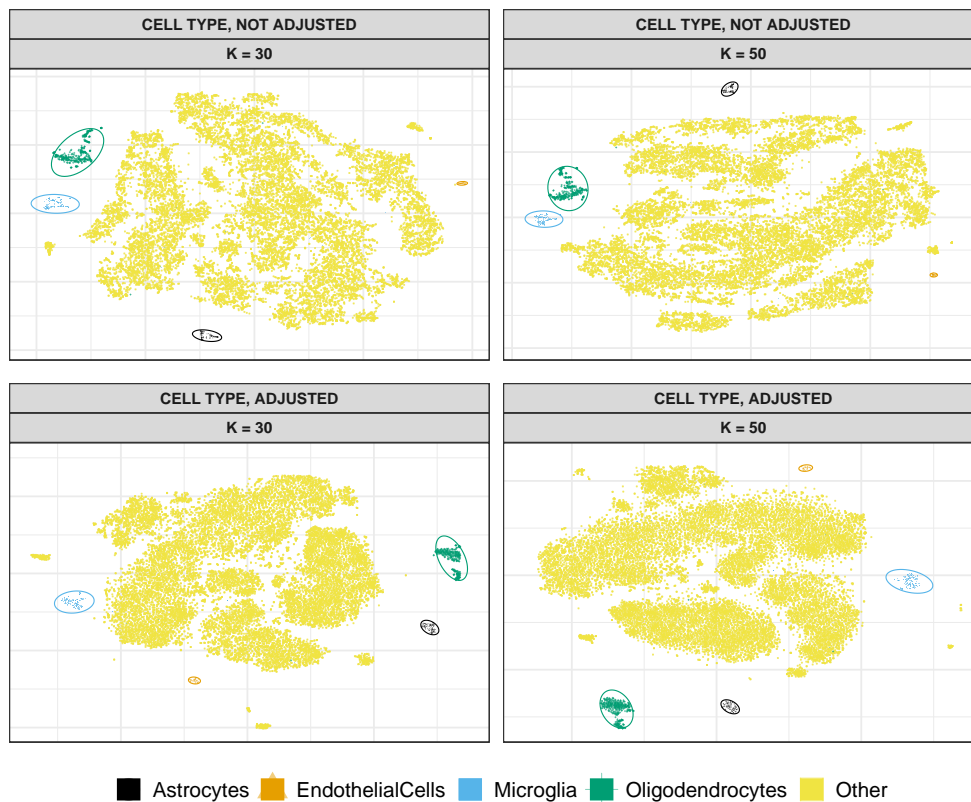


Figure 4: t -SNE coordinates after adjustment. Points and shapes vary with cell types.

systematic variations are not associated with any batch variables described before. Such batches are marked by the color and shape of points in Figure 3, showing that the batches are spread homogeneously across the embedded space after adjustment.

After removing batch effects, it is important to check if clusters of cell types associated with medulloblastoma are preserved in the low-dimensional coordinates. Current empirical findings are consistent with such a concern, as illustrated in Figure 4 which shows results for the unadjusted t -SNE in the upper panels and for the proposed method in the bottom ones. For both methods, the bulk of cells in a large central cluster are from tumors having markers within in a range of differentiation states, ranging from proliferative, undifferentiated cells expressing the SHH-pathway transcription factor *Gli1*, to cells in successive states of CGN differentiation, marked by sequential expression of markers *Ccnd2*, *Barhl1*, *Cntn2*, *Rbfox3*, and *Grin2b*. Clusters of cells surrounded with colored ellipses correspond to endothelial cells, microglia, oligodendrocytes and astrocytes, which are common in the stroma within or adjacent to the tumors. Empirical findings suggest that such clusters are correctly preserved after adjustment.

5 DISCUSSION

In this article we have introduced BC- t -SNE, a novel modification of t -SNE which allows to correct for multiple batch effects during estimation of the low-dimensional embeddings. The proposed approach has demonstrated good performance in simulation studies and on an application involving mouse medulloblastoma, where unwanted

variations are successfully removed without affecting cell types information.

A possible extension for future developments involves adapting the proposed procedure to more efficient optimisation of the t -SNE loss function, to overcome the computational constraints encountered with large n (Maaten, 2014). One way to address such an issue involves the use of alternative gradient methods, with methods based on stochastic gradients being popular in the literature.

Although visual inspection of t -SNE embeddings provides interesting insights on the low-dimensional structure of scRNAseq data, in many applications it is important to explicitly provide clusters of cells, which are often estimated on the resulting t -SNE coordinates via standard algorithms (e.g. k -means). An interesting direction to improve estimation is to include clusters estimation during t -SNE optimisation, providing a joint model for clustering and positions which allows one to take into account more carefully local similarities among points belonging to the same clusters in the low-dimensional space.

FUNDING

The work of Emanuele Aliverti and David B. Dunson was partially funded by the grant “Fair predictive modelling” from the Laura & John Arnold Foundation. We thank the UNC CGBID Histology Core supported by P30 DK 034987, the UNC Tissue Pathology Laboratory Core supported by NCI CA016086 and UNC UCRF, and the UNC Neuroscience Center Confocal and Multiphoton Imaging and bioinformatics cores supported by The Eunice Kennedy Shriver National Institute of Child Health and Human Development (U54HD079124) and NINDS (P30NS045892). J.O. was supported by NINDS (F31NS100489). T.R.G. was supported by NINDS (R01NS088219, R01NS102627, R01NS106227) and by the UNC Department of Neurology Research Fund. T.R.G., K.W., and B.B. were supported by a TTSA grant from the NCTRACS Institute, which is supported by the National Center for Advancing Translational Sciences (NCATS), National Institutes of Health, through Grant Award Number UL1TR002489.

REFERENCES

- Aliverti, E., Lum, K., Johndrow, J. E., and Dunson, D. B. (2018). Removing the influence of a group variable in high-dimensional predictive modelling. *arXiv preprint arXiv:1810.08255*.
- Alter, O., Brown, P. O., and Botstein, D. (2000). Singular value decomposition for genome-wide expression data processing and modeling. *Proceedings of the National Academy of Sciences*, 97(18):10101–10106.
- Benito, M., Parker, J., Du, Q., Wu, J., Xiang, D., Perou, C. M., and Marron, J. S. (2004). Adjustment of systematic microarray data biases. *Bioinformatics*, 20(1):105–114.
- Bylesjö, M., Eriksson, D., Sjödin, A., Jansson, S., Moritz, T., and Trygg, J. (2007). Orthogonal projections to latent structures as a strategy for microarray data normalization. *BMC bioinformatics*, 8(1):207.

- Ellison, D. W., Dalton, J., Kocak, M., Nicholson, S. L., Fraga, C., Neale, G., Kenney, A. M., Brat, D. J., Perry, A., Yong, W. H., et al. (2011). Medulloblastoma: clinicopathological correlates of shh, wnt, and non-shh/wnt molecular subgroups. *Acta neuropathologica*, 121(3):381–396.
- Hastie, T., Tibshirani, R., and Wainwright, M. (2015). *Statistical learning with sparsity: the lasso and generalizations*. Chapman and Hall/CRC.
- Helms, A. W., Abney, A. L., Ben-Arie, N., Zoghbi, H. Y., and Johnson, J. E. (2000). Autoregulation and multiple enhancers control math1 expression in the developing nervous system. *Development*, 127(6):1185–1196.
- Hinton, G. E. and Roweis, S. T. (2003). Stochastic neighbor embedding. In *Advances in neural information processing systems*, pages 857–864.
- Hwang, B., Lee, J. H., and Bang, D. (2018). Single-cell rna sequencing technologies and bioinformatics pipelines. *Experimental & molecular medicine*, 50(8):96.
- Johnson, W. E., Li, C., and Rabinovic, A. (2007). Adjusting batch effects in microarray expression data using empirical bayes methods. *Biostatistics*, 8(1):118–127.
- Krijthe, J. H. (2015). *Rtsne: T-Distributed Stochastic Neighbor Embedding using Barnes-Hut Implementation*. R package version 0.15.
- Kruskal, J. B. (1964). Multidimensional scaling by optimizing goodness of fit to a nonmetric hypothesis. *Psychometrika*, 29(1):1–27.
- Lazar, C., Meganck, S., Taminau, J., Steenhoff, D., Coletta, A., Molter, C., Weiss-Solis, D. Y., Duque, R., Bersini, H., and Nowé, A. (2012). Batch effect removal methods for microarray gene expression data integration: a survey. *Briefings in bioinformatics*, 14(4):469–490.
- Lee, J. A. and Verleysen, M. (2005). Nonlinear dimensionality reduction of data manifolds with essential loops. *Neurocomputing*, 67:29–53.
- Leek, J. T. and Storey, J. D. (2007). Capturing heterogeneity in gene expression studies by surrogate variable analysis. *PLoS genetics*, 3(9):e161.
- Luo, J., Schumacher, M., Scherer, A., Sanoudou, D., Megherbi, D., Davison, T., Shi, T., Tong, W., Shi, L., Hong, H., et al. (2010). A comparison of batch effect removal methods for enhancement of prediction performance using maqc-ii microarray gene expression data. *The pharmacogenomics journal*, 10(4):278.
- Maaten, L. v. d. (2014). Accelerating t-sne using tree-based algorithms. *The Journal of Machine Learning Research*, 15(1):3221–3245.

- Maaten, L. v. d. and Hinton, G. (2008). Visualizing data using t-sne. *Journal of machine learning research*, 9(Nov):2579–2605.
- Machold, R. and Fishell, G. (2005). Math1 is expressed in temporally discrete pools of cerebellar rhombic-lip neural progenitors. *Neuron*, 48(1):17–24.
- Macosko, E. Z., Basu, A., Satija, R., Nemesh, J., Shekhar, K., Goldman, M., Tirosh, I., Bialas, A. R., Kamitaki, N., Martersteck, E. M., et al. (2015). Highly parallel genome-wide expression profiling of individual cells using nanoliter droplets. *Cell*, 161(5):1202–1214.
- Mao, J., Ligon, K. L., Rakhlin, E. Y., Thayer, S. P., Bronson, R. T., Rowitch, D., and McMahon, A. P. (2006). A novel somatic mouse model to survey tumorigenic potential applied to the hedgehog pathway. *Cancer research*, 66(20):10171–10178.
- Pedregosa, F., Varoquaux, G., Gramfort, A., Michel, V., Thirion, B., Grisel, O., Blondel, M., Prettenhofer, P., Weiss, R., Dubourg, V., Vanderplas, J., Passos, A., Cournapeau, D., Brucher, M., Perrot, M., and Duchesnay, E. (2011). Scikit-learn: Machine learning in Python. *Journal of Machine Learning Research*, 12:2825–2830.
- Roweis, S. T. and Saul, L. K. (2000). Nonlinear dimensionality reduction by locally linear embedding. *science*, 290(5500):2323–2326.
- Rubin, L. L. and de Sauvage, F. J. (2006). Targeting the hedgehog pathway in cancer. *Nature reviews Drug discovery*, 5(12):1026.
- Scherer, A. (2009). *Batch effects and noise in microarray experiments: sources and solutions*, volume 868. John Wiley & Sons.
- Tenenbaum, J. B., De Silva, V., and Langford, J. C. (2000). A global geometric framework for nonlinear dimensionality reduction. *science*, 290(5500):2319–2323.
- Vladoiu, M. C., El-Hamamy, I., Donovan, L. K., Farooq, H., Holgado, B. L., Ramaswamy, V., Mack, S. C., Lee, J. J., Kumar, S., Przelicki, D., et al. (2018). Childhood cerebellar tumors mirror conserved fetal transcriptional programs. *bioRxiv*, page 350280.
- Wall, M. E., Rechtsteiner, A., and Rocha, L. M. (2003). Singular value decomposition and principal component analysis. In *A practical approach to microarray data analysis*, pages 91–109. Springer.
- Zappia, L., Phipson, B., and Oshlack, A. (2018). Exploring the single-cell rna-seq analysis landscape with the scrna-tools database. *PLoS computational biology*, 14(6):e1006245.
- Zurawel, R. H., Allen, C., Chiappa, S., Cato, W., Biegel, J., Cogen, P., de Sauvage, F., and Raffel, C. (2000). Analysis of ptch/smo/shh pathway genes in medulloblastoma. *Genes, Chromosomes and Cancer*, 27(1):44–51.